Functionalized graphene oxide-based waterborne hyperbranched polyester nanocomposite

Highlights

Present chapter deals with the development of high performing waterborne hyperbranched polyester (WHPE) nanocomposite with graphene oxide (GO). The homogeneously dispersed GO in WHPE matrix with controlled interfacial interaction is the daunting challenge owing to the presence of strong cohesive energy in both. Thus, in this study GO was functionalized with toluene diioscyanate (TDI) and butane diol (BD) through a simple method and subsequently incorporated into the WHPE matrix through a facile *in-situ* bulk polymerization technique without using any compatibilizing agent or organic solvent. The thermoset of the nanocomposite was formed by curing it with glycerol based hyperbranched epoxy (HBGE) and poly(amido amine) (PAA). The resultant thermosetting nanocomposites with 0.1-1 wt% functionalized GO (f-GO) exhibited significant enhancement in mechanical properties like elongation at break, tensile strength, scratch hardness, toughness, Young's modulus and impact resistance as well as thermal properties. The nanocomposite was also biodegradable under exposure of *Pseudomonus argeunosa* bacterial strain. Furthermore, it exhibited strong catalytic activity for Aza-Michael addition reaction. Thus, the nanocomposite can be utilized as a high performing sustainable material in different potential applications including heterogeneous catalysis.

This chapter is published in

Hazarika, D., Gupta, K., Mandal, M., and Karak, N. High performing biodegradable waterborne polyester/functionalized graphene oxide nanocomposites as an ecofriendly marterial. *ACS Omega,* 3(2):2292-2303, 2018.

3.1. Introduction

It is discussed in **Chapter 1** that nanotechnology is a multidisciplinary field which involves design, engineered and fabrication of devices at the nanoscale with significantly alternative and enhancing material properties [1]. The combined effect of nano reinforcing material and polymer matrix leads to development of high performing polymeric materials for various industrial applications as mentioned in **Chapter 1**, through enhancement of mechanical, thermal, optical, electronic, magnetic, etc. properties [2]. Typical reinforcement phase include clay, carbon nanotubes, metal oxide nanoparticles, graphene and its derivatives, etc. [3-5]. Graphene is gaining greater attention among them owing to its excellent mechanical properties, high aspect ratio, outstanding electrical and thermal conductivity, high surface area, etc. Further, unique structure of it opens up a new avenue to fabricate more efficient devices for various applications [6, 7]. GO contains a variety of reactive oxygeneous functional groups like hydroxyl, epoxy, and carboxylic acid compared to graphene and thereby facilitates fabrication process. It is readily form aqueous dispersion as well as dispersible in various organic solvents and even in polymers, and the functional groups of it may interact with polyester matrix [7]. However, as the number of such polar functional groups in GO is very large which interact among themselves so strongly that the interaction with the polymer matrix is a genuine question. Therefore, to improve such interactions some of the polar functional groups of GO may be functionalized with appropriate reactants to facilitate better interactions with the polyester matrix and results uniform dispersion in the polymer matrix [8, 9]. This f-GO is thought to be an ideal nano reinforcing agent for WHPE, because the oxygeneous groups of GO like hydroxyl and epoxide spreading across the basal planes, and carbonyl groups existing at edge sites facilitate the dispersion and interaction with the matrix, thereby helping in exfoliation of GO. Further, the fabrication of nanocomposite of WHPE with GO can also address the shortcomings of pristine polyester system from low mechanical, thermal properties, etc., and thereby facilitating their applications in various advanced fields. Further, apart from enhancement in these properties, incorporation GO also retained biodegradability of the material. To date, a relatively restricted number of studies was reported on polyester/GO nanocomposite and no report was available in literature on incorporation of GO in bio-based WHPE system, so far. In literature, Bastiurea *et al.* [10] studied mechanical and thermal properties of polyester nanocomposite with GO and graphene but the reported

properties were not up to the mark. Further, fabrication of unsaturated polyester and GO nanocomposite was reported by Bora *et al.* [11] and the studied mechanical and thermal properties of this nanocomposite, especially elongation at break was found to be very low. He *et al.* [12] reported the thermal properties and fracture toughness of an unsaturated polyester/GO nanocomposite. However, mechanical properties of all the reported polyester /GO nanocomposites are found to be poor to meet the requirement for any advanced applications. Further, all of the reported literature used large amounts of organic solvents for fabrication of nanocomposites which are not attractive for industrial production. Furthermore, on the basis of literature report on Aza-Michael addition reaction using GO [13], herein we report the fabrication of novel waterborne polyester supported f-GO catalyst and its use for Aza-Michael reaction in water, a greener solvent to achieve a complete environmentally friendly process. The utilization of environmentally benign solvents and materials signifies an ideal greener chemical technological process from both economic and environmental viewpoints.

Therefore, in the present work, WHPE nanocomposites were fabricated with different loading of f-GO through an organic solvent and compatibilizing agent free *in- situ* polymerization technique to obtain high performing eco-friendly material. The mechanical, thermal, biodegradation, etc. properties of the thermosetting nanocomposite were also studied. The catalytic activity of the nanocomposite for Aza-Michael addition reaction was also evaluated along with its recyclability to judge the efficiency as a heterogeneous catalyst.

3.2. Experimental

3.2.1. Materials

Citric acid-based WHPE was chosen in this study owing to their ease of preparation, low cost, single step process and biodegradability. Here, WHPE50 was used as the matrix for fabrication of the nanocomposite due to the overall best performance among other WHPE thermosets as mentioned in **sub-chapter 2B**. Thus, the materials and processes involved related to WHPE50 in this study are same as described in **sub-chapter 2B**.

HBGE used for fabrication of thermosetting nanocomposite was prepared by the same method as described in **sub-chapter 2A, sub-section 2A.2.3.**1. PAA was also the same grade as mentioned in **sub-Chapter 2A, sub-section 2A.2.1** and used for preparation of the thermosets.

Graphite flakes (60 mesh) used as the precursor for preparation of GO were procured from Loba Chemie, India with 99% purity.

Potassium permanganate ($KMnO_4$) with molar mass 158.03 g mol^{-1}, density 2.70 g cm^{-3} and melting point 240 °C was purchased from Analytical Rasayan, India. In this study,it was used as an oxidizing agent for the preparation of GO.

Sulphuric acid (H_2SO_4) was obtained from Merck, India with molar mass 98.08 g mol^{-1} and used in this study for the oxidation of graphite.

Hydrogen peroxide (H_2O_2) was purchased from Merck, India with molecular weight 34.015 g mol^{-1}, melting point -0.43 °C and boiling points 150.2 °C. It is a strong oxidizing agent and industrially formed by the hydrolysis of ammonium peroxydisulfate. Here, it was used to reduce the residual permanganate and manganese dioxide to colorless water soluble manganese salt.

Hydrochloric acid (HCl) used for washing and removing of excess manganese salt from GO was the same grade as mentioned in **sub-Chapter 2A, sub-section 2A.2.1**.

TDI used for functionalization of GO was purchased from Merck, Germany with molar mass 174.16 g mol^{-1}, density 1.22 g cm^{-3}, boiling point 247 °C and melting point 12-14 °C.

1, 4-BD was achieved from Merck, Germany and used as a reactant in this study for functionalization of GO. The molar mass, melting point, boiling point and density of it are 90.12 g mol^{-1}, 20 °C, 228 °C and 1.02 g cm^{-3} respectively.

Diethyl amine used as a reactant for Aza-Michael addition reaction was obtained from Merck, India.

Acrylonitrile was purchased from Merck, India and used in this study as one of the reactants of Aza-Michael addition reaction. The molar mass, boiling point and density of it are 53.06 g mol^{-1}, 77.3 °C and 0.81 g cm^{-3} respectively.

Methyl methacrylate was also used in Aza-Michael reaction and obtained from Merck, India with molar mass 100.12 g mol^{-1}, boiling point 101 °C and density 0.94 g cm^{-3}.

Aniline was achieved from Merck, India with molar mass 93.13 g mol^{-1} and used as a reactant of Aza-Michael reaction. The boiling point and density of it are 184 °C and 1.02 g cm^{-3} respectively.

3.2.2. Characterization

FTIR, NMR, TGA, DSC and SEM analyses were carried out under the same conditions

as stated in **sub-chapter 2A, sub-section 2A.2.2**, by using the same instrumental specifications. An ultrasonicator (UP200S, Hielscher Ultrasonics GmBH, Germany) at amplitude of 60% with 0.5 cycle was used to disperse GO in water. It was operated at a frequency of 24 kHz with a standard sonotrode (tip-diameter 3 mm). Here, Raman spectra of GO and f-GO were taken with Renishaw, UK. An X-ray diffraction (XRD) (Bruker AXS, D8 FOCUS, Germany) study was conducted for GO, f-GO and the nanocomposite.

Further, the morphology, structure and selected area electron diffraction (SAED) patterns of GO, f-GO and the nanocomposite were analyzed by high resolution transmission electron microscope (HRTEM, JEOL 2100X) at an operating voltage of 200 kV. High magnification images were captured by preparing a very dilute dispersion of the nanocomposite in THF and mounted on a carbon coated copper grid. f-GO was dispersed in THF by using an ultrasonicator with the same specification as stated in characterization part. Tensile strength, elongation at break, scratch hardness and impact resistance of the nanocomposite were studied by using the same instruments under the same test conditions as mentioned in **sub-Chapter 2A, section 2A.2.2**.

Further, the well-established Halpin-Tsai model was utilized for prediction of Young's modulus of the nanocomposite, where the reinforcing agent distributed either randomly or parallel [14, 15]. The same may be employed for prediction of Young's modulus of graphene based nanocomposites where graphene nanosheets may aligned parallel or distributed randomly. To estimate the Young's modulus of such nanocomposite the following equations were utilized [14, 15]. **Eq. 3.1** and **Eq. 3.2** were used for randomly distributed and parallely aligned nanosheets based nanocomposites respectively.

$E_{NC} = E_P [3/8\{(1 + \eta_L\zeta V_C)/(1 - \eta_L V_C)] + 5/8 \{(1 + 2\eta_T V_C)/(1 - \eta_T V_C)\}]$ ……..(**Eq. 3.1**)

$E_{\parallel} = E_P [(1 + \eta_L\zeta V_C)/(1- \eta_L V_C)]$ ……..(**Eq. 3.2**)

where $\eta_L= [(E_{GO}/E_P-1)/(E_{GO}/E_P + \zeta)]$, $\eta_T = [(E_{GO}/E_P - 1)/ (E_{GO}/E_P + 2)]$ and E_{NC}, E_P and E_{GO} are the Young's modulus of the nanocomposite, pristine polyester and GO respectively, ζ is diameter to thickness ratio and V_C is volume fraction of GO. The density and Young's modulus GO are 2.2 g cm^{-3} and 215 GPa as reported in literature [14]. The density of WHPE is 1.12 g cm^{-3} as provided **in sub-chapter 2B**.

3.2.3. Preparation of GO

GO was prepared according to the well established Hummers method [6] by the oxidation of graphite using H_2SO_4 (concentrated) and $KMnO_4$. Briefly, 2 g of graphite powder in 35 mL of H_2SO_4 (98%) was placed in a single necked round bottom flask and stirred for 2 h. Then, $KMnO_4$ (6 g) was slowly added into the above solution by maintaining the temperature at less than 20 °C using an ice-bath and the mixture was stirred for 4 h at 35 °C. The resulting solution was diluted by stepwise addition of 90 mL of water under vigorous stirring and continued for 1 h. Then, a dark brown suspension was obtained and further treated by adding 30% H_2O_2 solution drop wise until the color of the solution became bright yellow. The resultant suspension of GO was centrifuged repeatedly and washed by dilute HCl (5%) solution to eliminate excess of manganese salt followed by water until the pH of the solution became neutral. Further, ultrasonically the exfoliated GO was made as water dispersible and for obtaining the dry GO powder, it was dried in a vacuum oven.

3.2.4. Functionalization of GO

Functionalization was done by reacting GO with a requisite amount of TDI and BD. In brief, 0.5 g of GO was dispersed in 25 mL of THF by mechanical shearing followed by sonication. The dispersed GO was placed in a three-necked flask outfitted with a Teflon septum, a mechanical stirrer and a nitrogen gas inlet. TDI (0.82 mmol) was added dropwise into the above GO suspension at room temperature. The reaction was again continued at 70 ± 4 °C for 2-3 h to achieve the isocyanate terminated GO. Then, BD (0.41 mmol) was added into the above mixture and the reaction was further continued for another 1 h which resulted the desired functionalized GO (f-GO). The free reactants/components were separated by centrifuging and washing f-GO with THF. The obtained f-GO was dried in a vacuum oven.

3.2.5. Fabrication of WHPE/ f-GO nanocomposite

WHPE nanocomposites were fabricated by using different amounts of f-GO through an *in-situ* technique without using any compatibilizing agent and organic solvent. The first step of this fabrication process was same as the synthesis of pristine polyester as described in **sub-Chapter 2B, sub-sections 2B. 2.1**. In the second step, the requisite amount of bis-MPA and glycerol was added to it along with the required amount of f-GO

after cooling this reaction mixture to 60 °C and then again the reaction was carried out at 140 °C. This product can be diluted by water to the desired extent. Three different compositions of nanocomposites were fabricated using different wt% (0.1, 0.5 and 1) of f-GO by following the similar preparative protocol, and the nanocomposites are denoted as PFGN0.1, PFGN0.5 and PFGN1 respectively. The nanocomposite of polyester with GO (0.1 wt%) was also prepared for comparison purpose and coded as PGN0.1.

3.2.6. Preparation of the thermosets

The thermosets of this WHPE nanocomposite was prepared by following the same procedure as described in **sub-chapter 2A, sub-section 2A.2.3.3**.

3.2.7. Method for Aza-Michael addition reaction

The nanocomposite was tested as a heterogeneous catalyst for Aza-Michael addition reaction (**Scheme 3.1**). A mixture of 1.2 mmol of α, β-unsaturated compound and 1 mmol of amine substrate were stirred at room temperature in presence of 2.5×10^{-3} g of catalyst (PFGN1). The completion of the reaction was confirmed by TLC and the product was extracted from the reaction mixture using ethyl acetate. The catalyst was recovered by simple filtering after completion of the first cycle. Further, to check the recyclability of the catalyst for this reaction, a set of experiments was performed.

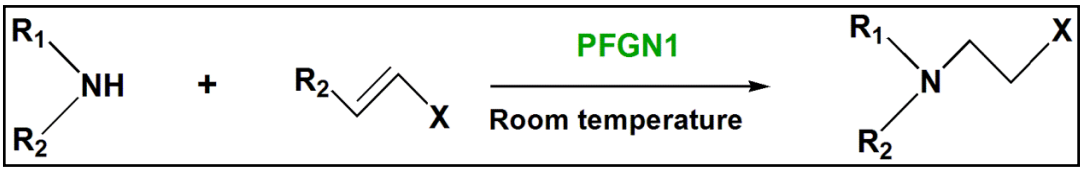

Scheme 3.1: PFGN1 catalyzed Aza-Michael addition reaction

3.2.8. Biodegradation study

Biodegradation study of the nanocomposite was carried out using *Pseudomonus aeruginosa* bacterial strain by following the same procedure as described in **sub-chapter 2A, sub-section 2A.2.8** under the same experimental condition.

3.3. Results and Discussion

3.3.1. Functionalization of GO

In the fabrication of WHPE/f-GO nanocomposite, key issues are dispersion of the nanomaterials and interfacial interactions of GO with the polyester matrix. The surface functionalization of GO is enormously influencing its state of dispersion in the polymer matrix. The oxygen containing functional groups including carboxylic acid, hydroxyl and epoxy groups can be used to change the surface functionality of GO [6, 16]. Thus, the functionalization of GO was achieved by the reaction of oxygenated functional groups of GO with isocyanate groups of TDI followed by reacting with BD and resulted isocyanate-terminated GO. As the isocyanate is highly reactive, thus the covalent functionalization was occurred by direct linkage of OH groups of GO with the isocyanate groups. A schematic preparation of f-GO is shown in **Scheme 3.2**. Stable dispersion of GO and f-GO was observed in different solvents such as THF, DMF, DMAc, DMSO, etc. (**Scheme 3.2)**.

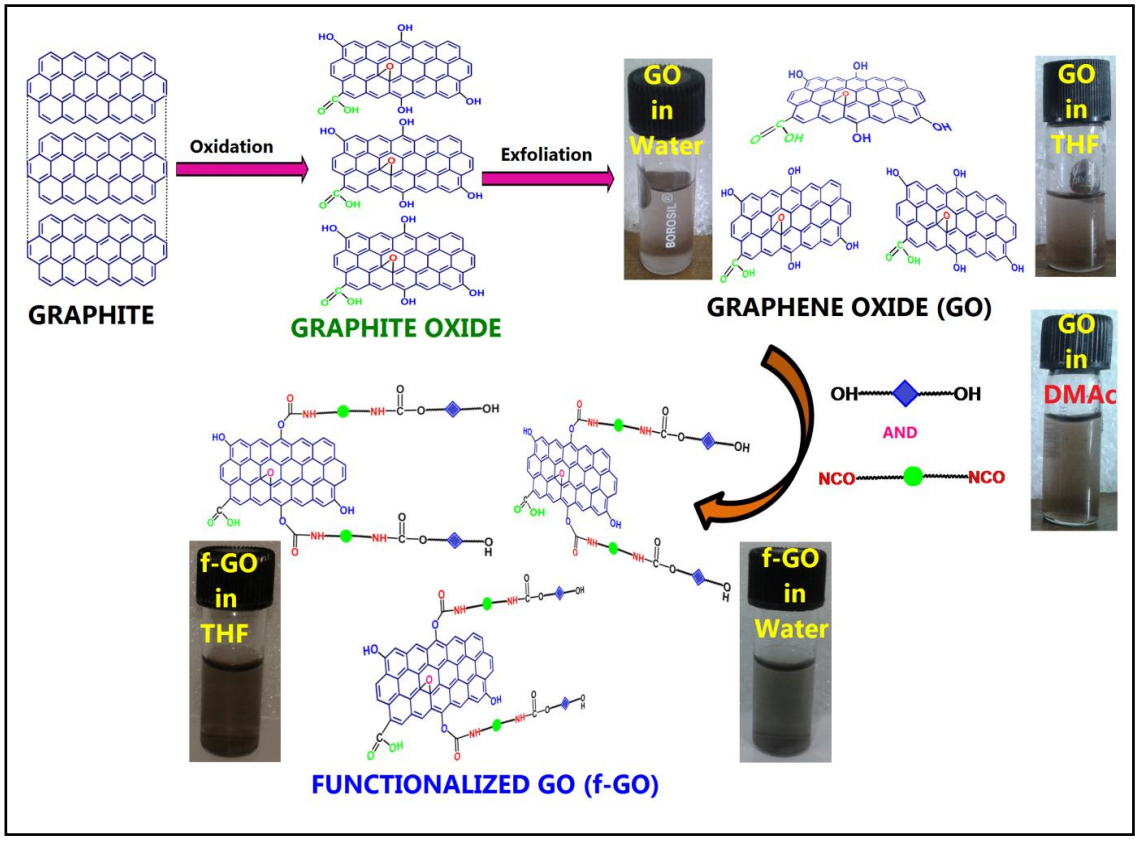

Scheme 3.2: Schematic route for functionalization of GO (f-GO) from graphite (Photos of GO and f-GO in different solvents)

3.3.2. Characterization

GO and f-GO were analyzed by different spectroscopic and diffraction techniques. FTIR is used to establish the presence of various oxygen-containing functional groups in them. In the FTIR spectrum of GO (**Figure 3.1a**), the occurrence of intense bands at 1720 cm^{-1} (-C=O stretching), 1202 cm^{-1} (-C–O–C stretching), 1047 cm^{-1} (-C–O stretching) and a broad band at 3402 cm^{-1} (-O-H stretching) indicate the occurrence of oxygeneous groups like carbonyl, carboxylic, epoxy and hydroxyl in it. The bands appeared in the range of 3000−2700 cm^{-1} are owing to the stretching vibrations of $-CH_2$ (symmetric and asymmetric) [6-8]. While FTIR spectrum (**Figure 3.1a**) of f-GO showed the presence of absorption frequencies at 1541, 1642, 1052, 1700 and 1217, cm^{-1} which are ascribed to the stretching vibrations of bending of -N−H of amide II, -C=C, -C−N, carbonyl of amide I and -C−O respectively [6]. Thus, this FTIR analysis confirmed the covalent bond formation with GO by TDI and BD.

Further, X-ray diffraction patterns (**Figure 3.1b**) of pristine GO showed two peaks at 10.1° and 43.2° for (002) and (001) graphitic planes respectively. The peak at 10.1° is due to the presence of abundant oxygeneous groups which is similar to the reported literature [6, 7]. The positions of XRD peaks are slightly shifted after functionalization of GO which support the modification of GO. Furthermore, Raman spectroscopy is also an important technique to characterize the carbonaceous materials with ordered or disordered structures. Raman spectra of both GO and f-GO showed two fundamental vibration bands in the range of 1200 to 1700 cm^{-1} **(Figure 3.1c**) [17].

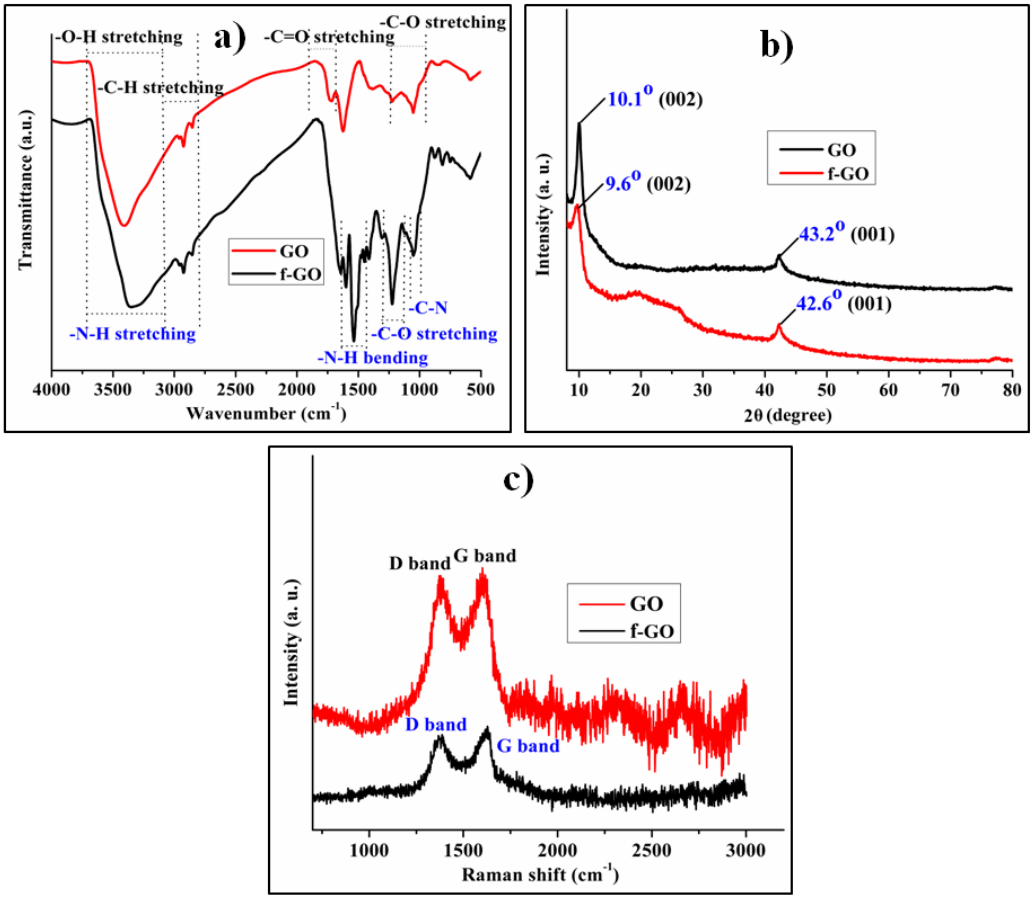

Figure 3.1: (a) FTIR spectra, **(b)** XRD patterns and **(c)** Raman spectra of GO and f-GO

The vibration mode at 1580 cm^{-1} (G) is due to the scattering (first-order) of E_{2g} phonons vibration of sp^2 carbon atoms and D vibration band (1351 cm^{-1}) is due to the A_{1g} breathing mode of carbon associated with structural defects and disorders [17].

Further, TEM analysis provides direct visualization of the morphology of GO and f-GO (**Figure 3.2a-d**). The exfoliated, transparent and wrinkled GO nanosheets and f-GO were observed from its TEM images with micrometers lateral dimension. The occurrence of topological features besides overlapping area of GO nanosheets revealed that they are extremely dispersed in water. According to the reported literature, the crumpled topology of GO is due to the presence of oxygeneous functional groups as well as extremely thin characteristic of the nanosheets [13, 18]. HRTEM image of f-GO further confirmed the retaining of layer structure of GO even after functionalization (**Figure 3.2e**). The selected area electron diffraction (SAED) pattern of f-GO is shown in **Figure 3.2f**.

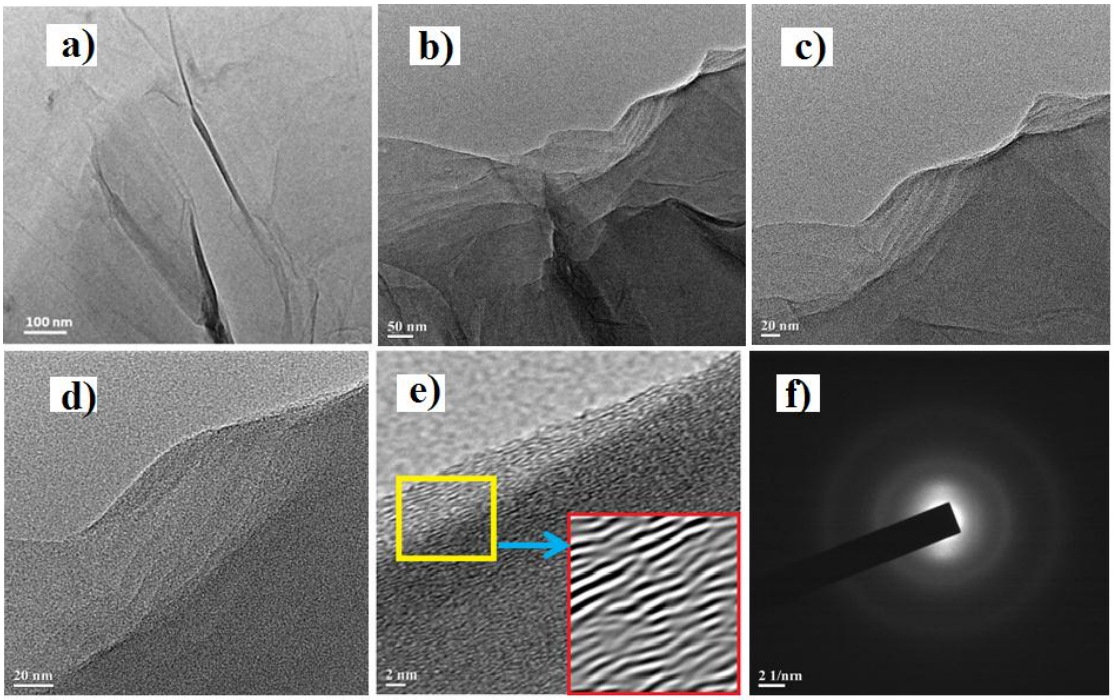

Figure 3.2: (a) TEM images GO and **(b)-(d)** TEM images of f-GO at different magnifications for morphological observation, **(e)** HRTEM images at 2 nm for layer observation and **(f)** SAED pattern of f-GO

3.3.3. Fabrication of WHPE and f-GO nanocomposite

As both the components, polyester and GO are compatible due to the presence of adequate number of polar functional groups, so there are strong interactions among the components which are shown in **Scheme 3.3**. This interaction also helps to stabilize the dispersed f-GO and the stable dispersion was achieved by mechanical shearing force followed by ultrasonication even in aqueous medium (**Scheme 3.3**). As ultrasonication generates a localized intensity with high pressure, temperature and energy, helps in the dispersion at nanoscale level. To fabricate WHPE/f-GO nanocomposite, *in-situ* polymerization technique was employed under bulk conditions without using any solvent or compatibilizing agent. The –OH groups of f-GO interact covalently and non-covalently with the polyester matrix during the fabrication process. The nanocomposite was well dispersed in water, ethanol, DMAc, DMSO, THF, etc.

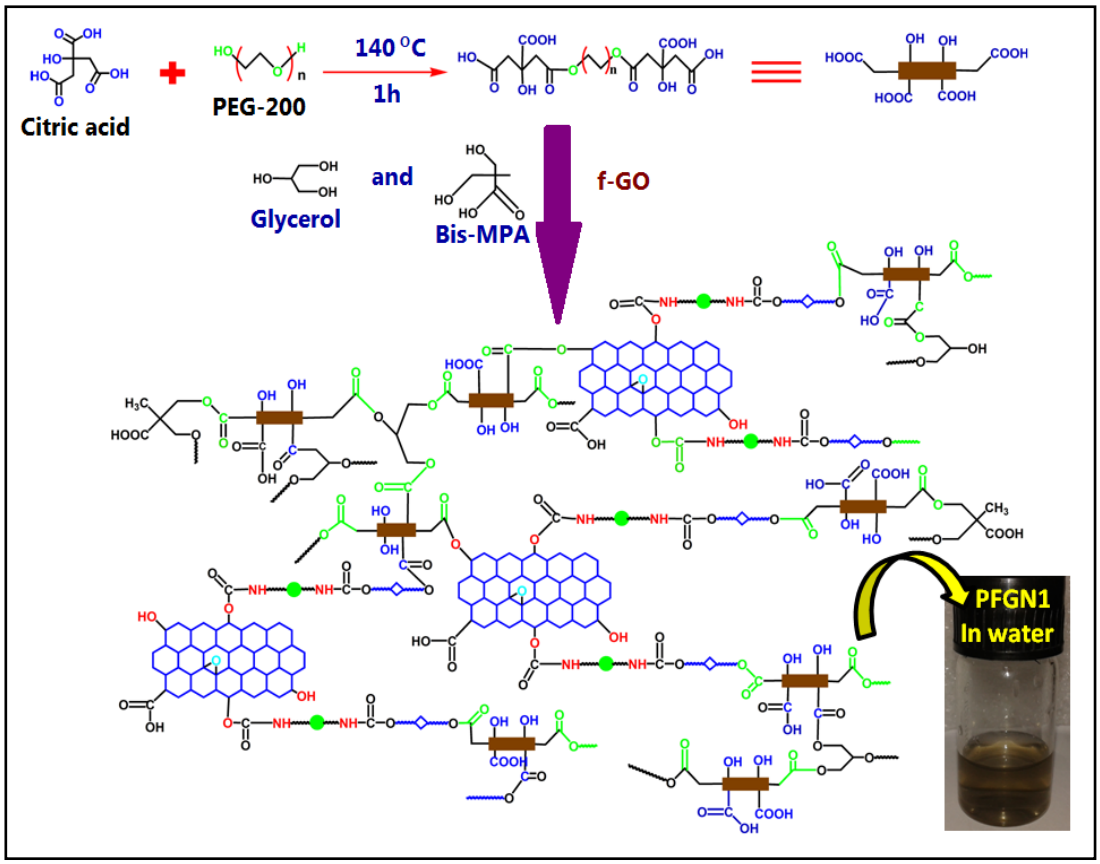

Scheme 3.3: Fabrication route of WHPE/f-GO nanocomposite

The resultant nanocomposite was characterized by various spectroscopic techniques such as FTIR, XRD and TEM. The characteristic absorbance bands for pristine polyester were found at 3451 cm^{-1} (-O-H stretching), 2953-2805 cm^{-1} (-C-H symmetric and asymmetric stretching) and 1739 cm^{-1} (-C=O stretching). The characteristic carbonyl peak for the ester group was slightly shifted after formation of the nanocomposite as observed from the FTIR spectrum of PFGN1 (**Figure 3.3a**). Further, the band at 3000-3500 cm^{-1} corresponding to the hydroxyl group of GO shifted to the lower wavenumber. The shifting of the bands as well as the decreased in intensities of carbonyl group usually considered as the evidence of hydrogen bond formation between the polyester matrix and f-GO [19]. Therefore, the shifting of peak positions in the FTIR spectrum of the nanocomposite (**Figure 3.3a)** indicates the existence of strong interactions such as polar-polar, hydrogen bonding, etc. between the polyester matrix and f-GO. Further, in the XRD pattern of PFGN0.5 (**Figure 3.3b)** a broad peak was observed in the range of 15-30° without the distinctive intense peak of f-GO. These peaks were disappeared in nanocomposites because of the strong interaction of finely dispersed f-GO with the polar functional groups of pristine polyester, hyperbranched epoxy and the

hardener which reduces its crystallinity as well as may be owing to masking effect since the quantity is very low [20].

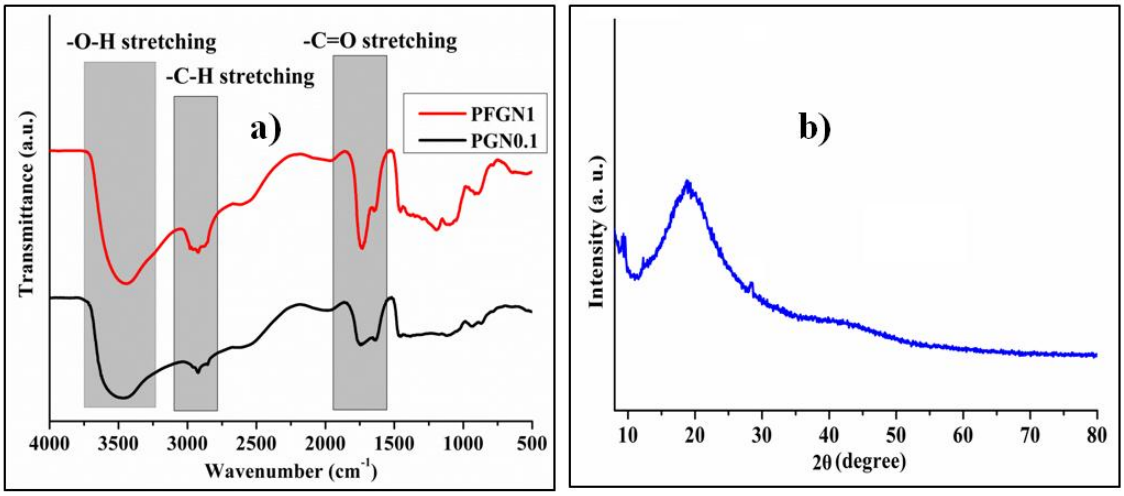

Figure 3.3: (a) FTIR spectra of PGN0.1 and PFGN1, and **(b)** representative XRD pattern of PFGN0.5

SAED pattern of PFGN1 (**Figure 3.4**) further confirmed the amorphous nature of f-GO in the nanocomposites. TEM analysis was performed in order to further explore the morphology and dispersion of GO in the polyester matrix. The well dispersion of the f-GO in the nanocomposite without any aggregation and the occurrence of thin layers of edge folded f- GO sheets were visualized from TEM micrograph of PFGN1 (**Figure 3.4, Figure 3.5)**. Further, SEM images of the fractured surface of the nanocomposite are shown in **Figure 3.5** which also provide dispersion characteristic of the f-GO in the polyester matrix.

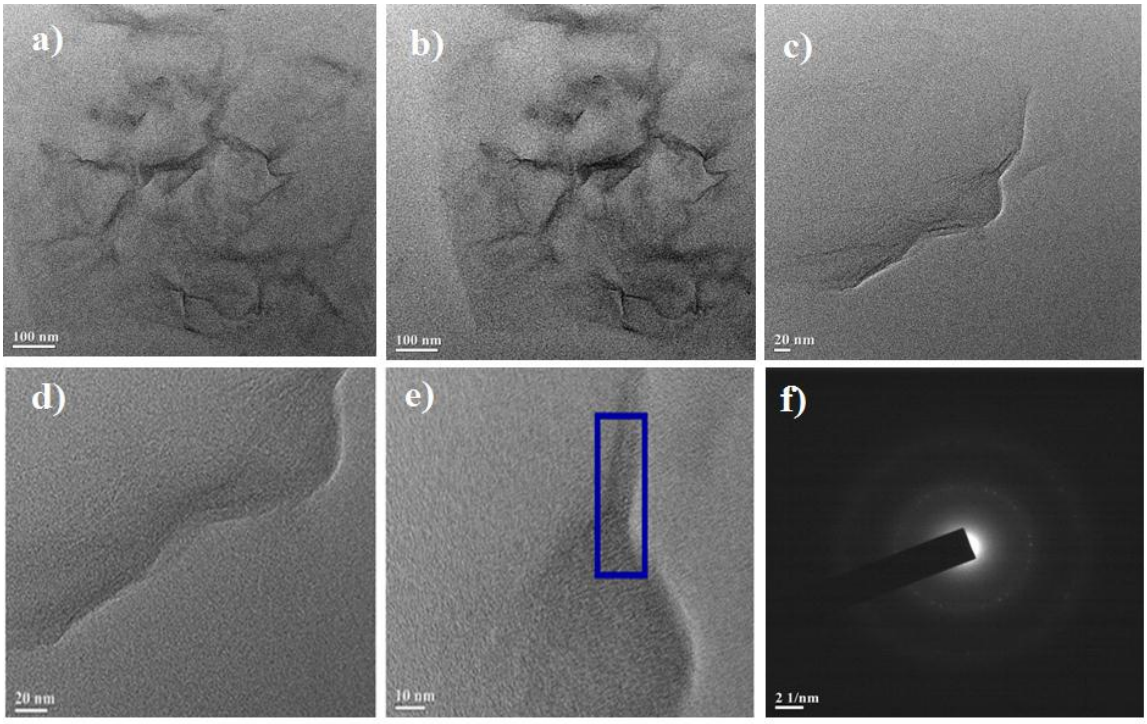

Figure 3.4: (a)-(d) Representative TEM images of PFGN1 at different magnification, **(e)** layer observation of f-GO in the nanocomposite and **(f)** SAED pattern

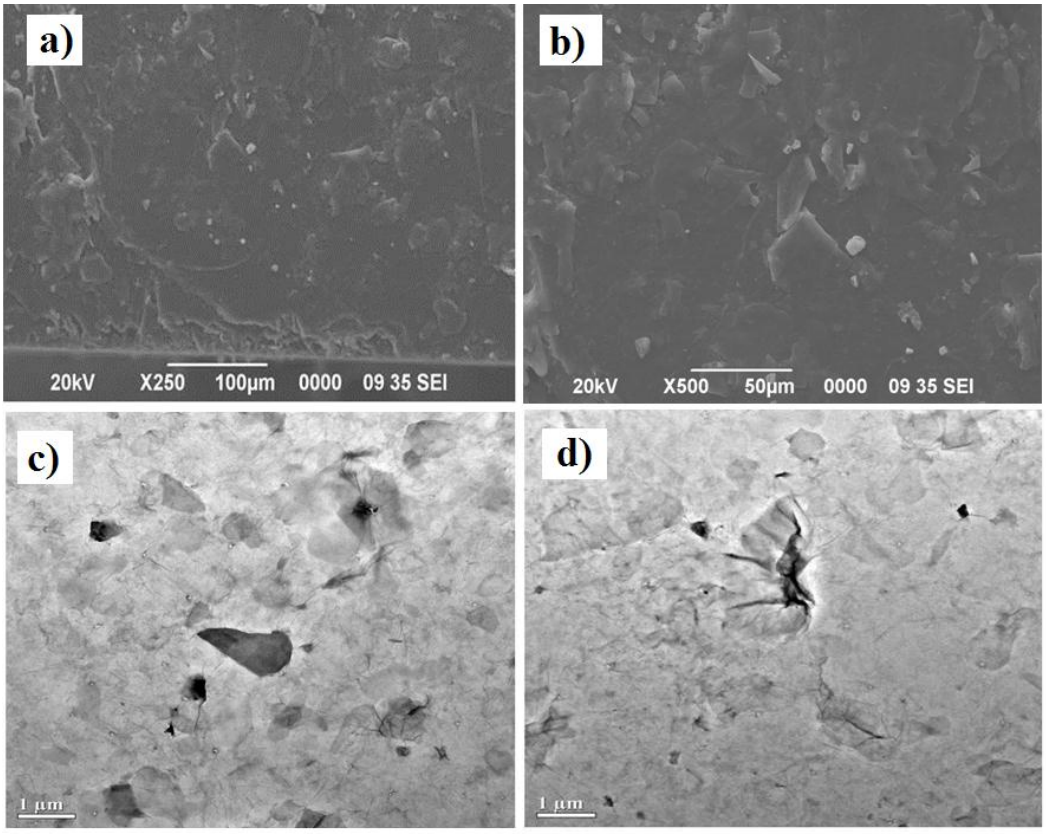

Figure 3.5: (a, b) SEM images of fractured surface of the nanocomposite and **(c, d)** TEM images of the nanocomposite under low magnification

3.3.4. Curing of the nanocomposite

The thermosets of polyester nanocomposite was obtained by curing it with HBGE and PAA at elevated temperature in a hot oven. The obtained films of nanocomposite were dark brown in color. The presence of varieties of reactive polar functional groups like hydroxyl, carboxylic, epoxy, etc. in the system made the mechanism of curing process complex. As a result, different reactions were occurred between them and the plausible cross-linking interactions are shown in **Scheme 3.4.** The primary amine groups of the hardener opened the epoxy ring of HBGE leading to the generation of secondary amine and –OH groups. The free hydroxyl groups of the nanocomposite were interacted with epoxide groups of HBGE [20, 21]. The hydrogen bonding was formed between -C=O of the polyester with the hydroxyl group of f-GO and HBGE. The transesterification reactions between ester and hydroxyl groups can also occur. Further, the free hydroxyl groups of f-GO and polyester interact with amino group of PAA.

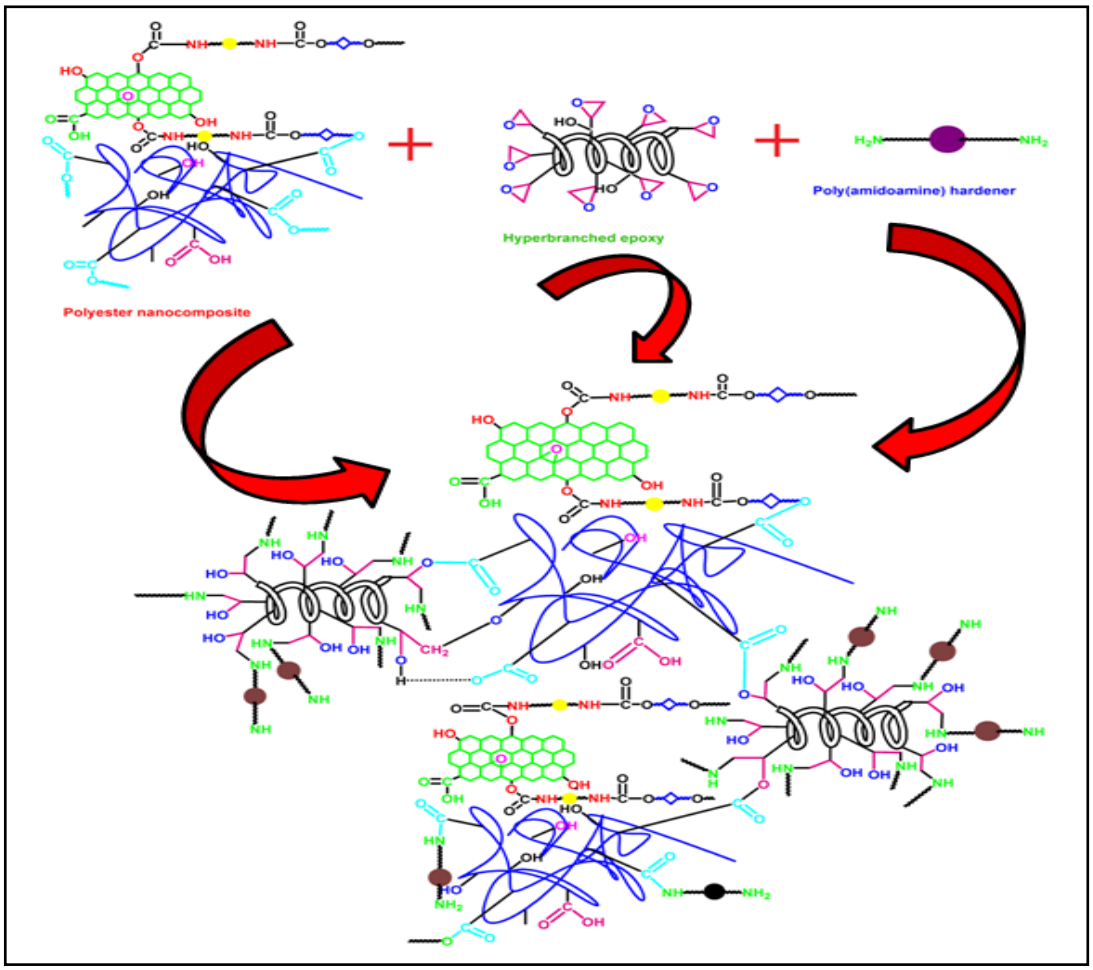

Scheme 3.4: Plausible interactions occurred during cross-linking reaction of the nanocomposite with HBGE and PAA

Furthermore, the etherification reaction of hydroxyl and epoxy may also take place. The different reactions among epoxide groups of HBGE, carboxylic and hydroxyl groups of the nanocomposite and f-GO; and amino groups of PAA could also be occurred [20, 21].

3.3.5. Performance characteristics

The main aim of incorporating GO into WHPE matrix is to address the poor mechanical properties of polyester. The factors such as particle-particle interaction and nanoparticle-matrix interaction play a key role in the performance of the nanocomposite. The attraction forces between particles influence the particle-particle interaction and weaken the performance of the nanocomposite. The attraction and repulsion forces can be controlled by particle size, particle volume fraction, particle surface modification, particle weight fraction, etc. [18]. The enhanced mechanical properties can be achieved through stronger interfacial interaction between nanomaterials and the polymer matrix [6, 22, 23]. The different mechanical properties such as scratch hardness, tensile strength, elongation at break, impact resistance, toughness, etc. of WHPE and WHPE/f-GO nanocomposite with different loadings of f-GO were evaluated and the values are summarized in **Table 3.1**. The stress-stain profiles of the nanocomposite (**Figure 3.6a**) showed the relationship between f-GO loading and tensile strength of the nanocomposite. The mechanical behavior of the nanocomposites apparently exhibited an enhancing trend upon the loading f-GO. From this table it is seen that nanocomposite showed significant enhancement in tensile strength compared to the pristine polyester. The enhancement can be ascribed to the well dispersion of f-GO in the polyester matrix and the existence of covalent bonding among polyester matrix and f-GO along with various secondary interactions. These help to construct strong interfacial interactions between polyester matrix and homogeneously dispersed f-GO. The presence of such interactions resulted partially restricted polymer phase and the orientation of polymer chain and f-GO along the route of tensile flow, offers a great involvement to the observed enrichment of the tensile strength. Further, these properties were found to be dose dependent and the values increased with increasing in the loading of f-GO. Increase in particle loading leads to creation of more nano-dimensional interface that may generate a strong polymer network enhancing the mechanical properties. Nanocomposite with the highest f-GO loading (1 wt%) exhibited the highest tensile strength (39 MPa), corresponding to an enhancement of 5 times to pristine polyester. The values were higher than that of reported polyester resin/GO [11] and epoxy/GO [24], etc. nanocomposites.

Table 3.1: Performance characteristics of the nanocomposites

Property	**PFGN0**	**PGN0.1**	**PFGN0.1**	**PFGN0.5**	**PFGN1**
Swelling value (%)	22 ± 1	23 ± 1	22 ± 2	22 ± 2	21 ± 1
Curing time (h)	5 ± 0.03	4.8 ± 0.5	4.6 ± 0.05	4.5 ± 0.02	4.3 ± 0.01
Tensile strength (MPa)	7.8 ± 1.5	11.7 ± 1	16.3 ± 1.6	29.1 ± 2	39.4 ± 2.5
Elongation at break (%)	245 ± 2	167 ± 3	273 ± 2	320 ± 2	360 ± 3
Scratch hardness (kg)*	4 ± 0.1	6 ± 0.1	8 ± 0.2	>10	>10
Impact resistance (kJm^{-1})*	>8.3	>8.3	>8.7	>8.8	>9.3
Toughness (MJm^{-3})**	17.2 ± 1.5	18.5 ± 2	36.2 ± 2.2	61.4 ± 2.4	86.4 ± 3
Gloss (°)	80 ± 2	85 ± 1	90 ± 3	94 ± 2	100 ± 2
Young's modulus (MPa)	243 ± 3	259 ± 2	266 ± 4	312 ± 3	358 ± 5

**The highest limit of the instrument, ** Calculated area under stress-strain curves*

Further, it is most interesting to observe that the nanocomposites not only exhibited higher tensile strength but also improved elongation at break over the pristine system. The values further increased with the increase in the loadings of f-GO in the nanocomposites. This increment is owing to the slippage of the graphene sheets when they are directly linked to the polymeric chains as shown in **Scheme 3.5**. In addition, on application of extended tensile force the immobilized or partially mobilized polymeric chains are able to elongate fully, and hence a good enrichment of elongation can be monitored. The values of elongation at break were found to be higher than the literature reported nanocomposites of polyester/GO [11], epoxy/ GO [24] and knit polyester fabric/GO [25], etc. Furthermore, toughness of the nanocomposite as calculated from the stress-strain curve was also enhanced. This is the result of combined effect of strength and flexibility, and the values were also increased with the loading of f-GO. Further, other mechanical properties like impact resistance as well as scratch hardness of the nanocomposite were also found to be enhanced. The enhanced mechanical properties

could be owing to the good interfacial interactions upon the homogeneous dispersion of f-GO in the polyester matrix. There is a chance of direct linkages among various oxygen containing groups of f-GO and the polyester by physicochemical interactions. This significantly enhances the compatibility of f-GO with the polyester matrix, which facilitates the direct transfer stress to f-GO from the matrix. This improves the strength of the nanocomposite. Furthermore, values of Young's modulus are calculated from the slope of the elastic region of the stress-strain curves and the values are given in **Table 3.1**. On introduction of f-GO, the values of Young's modulus were found to be enhanced due to chain stiffening effect which is further increased with the loadings of f-GO. Further, Young's modulus of the WHPE nanocomposites were calculated using **Eq. 3.1** and **Eq. 3.2** and compared with the experimentally obtained results at different GO loadings as shown in **Figure 3.6b**. From this figure, it is clear that experimental modulus values are much closer to the theoretical results of parallely aligned nanosheets compared to randomly distribute ones. This result demonstrated that the graphene nanosheets in the studied nanocomposites are mostly aligned in parallel direction.

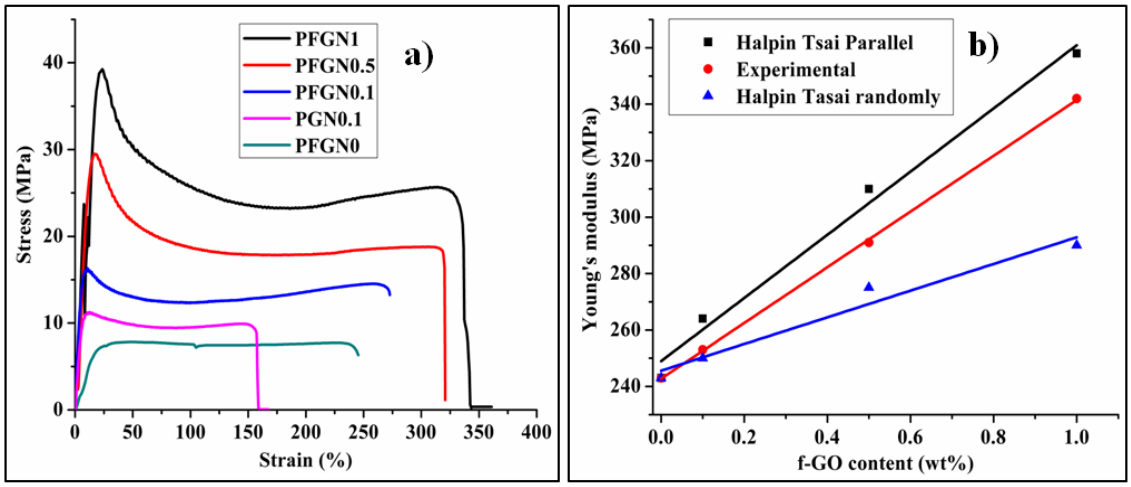

Figure 3.6: (a) Stress-strain profiles of the thermosets and **(b)** comparison between fitting results of Halpin–Tsai model and the experimental data

3.3.6. Thermal properties

The thermal behaviors of the nanocomposite as well as GO and f-GO are presented in **Figure 3.7a**. GO is thermally unstable owing to the presence of huge number of oxygeneous functional groups like carboxyl, carbonyl and hydroxyl and the TGA curve of it revealed a two-step degradation pattern (**Figure 3.7a**). The weight loss near 100 °C

is attributed to the evaporation of absorbed water molecules [6]. The first step degradation at 178 °C is owing to the loss of epoxy, hydroxyl and carboxylic groups as well as residual water molecules. The next step of degradation (430–520 °C) is due to the decomposition of the remaining oxygeneous functional groups yielding CO, CO_2 and H_2O vapors as well as the decomposition of ring carbon [6, 26]. The thermal degradation temperature of GO was slightly increase after functionalization which indicate that the thermally labile oxygeneous functional groups took part during functionalization process (**Figure 3.7a**). Further, the degradation temperature of the nanocomposites was shifted to temperature higher than that of the pristine system as well as f-GO (**Figure 3.7b**). This signifies good dispersion of the f-GO in the polyester matrix and strong interaction between them, and thereby resulting significant enrichment in the thermal stability. The thermostability of the nanocomposites was further enhanced with the increased f-GO loading.

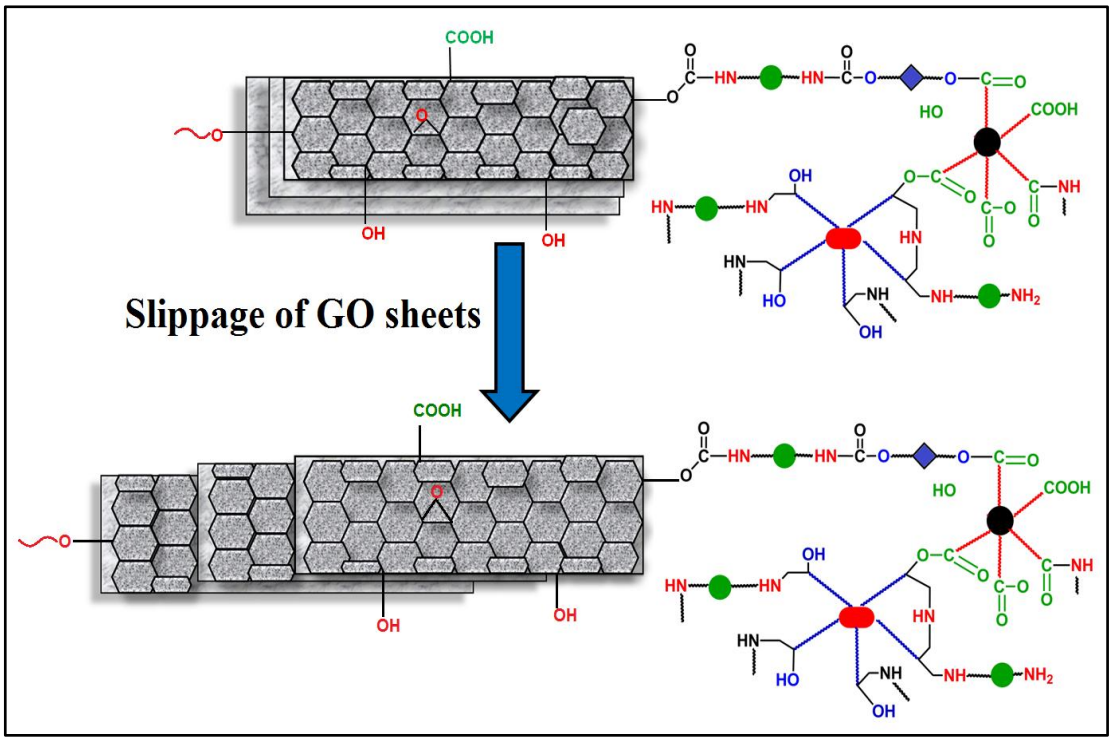

Scheme 3.5: Schematic representation of slippage of graphene layers

This is because of the fact that through the various physicochemical interactions with f-GO, the polymer chain motions are restricted. The enhancement in thermostability can be ascribed to the so-called ‘‘complicated path’’ effect of graphene platelets. GO acts as a barrier in polymer matrix to delay the escape of volatile degradation products and

retards the propagation of heat from the extraneous surroundings into the polyester matrix [6, 26].

Further, glass transition temperature (T_g) of the nanocomposite was evaluated from DSC analysis as shown in **Figure 3.7c**. The nanocomposite showed two different T_g, one in the range of 42-55 °C is due to α transition and another sub T_g at lower temperature (0-9 °C) is due to β-transition. The more confined polymer chains in the nanocomposites was achieved owing to the strong interfacial interaction which lead to a significant change in the T_g and contribute to detect the second glass transition. In α-transition local segments of polymer become mobile while β-transition is resulted because of the side group motions or other types of in-chain motion. This demonstrated as a measurable chain segmental motion which exists as a secondary relaxation process in the polymer chain. The segments like ester linkages and aliphatic moieties actually took part for such β-transition.

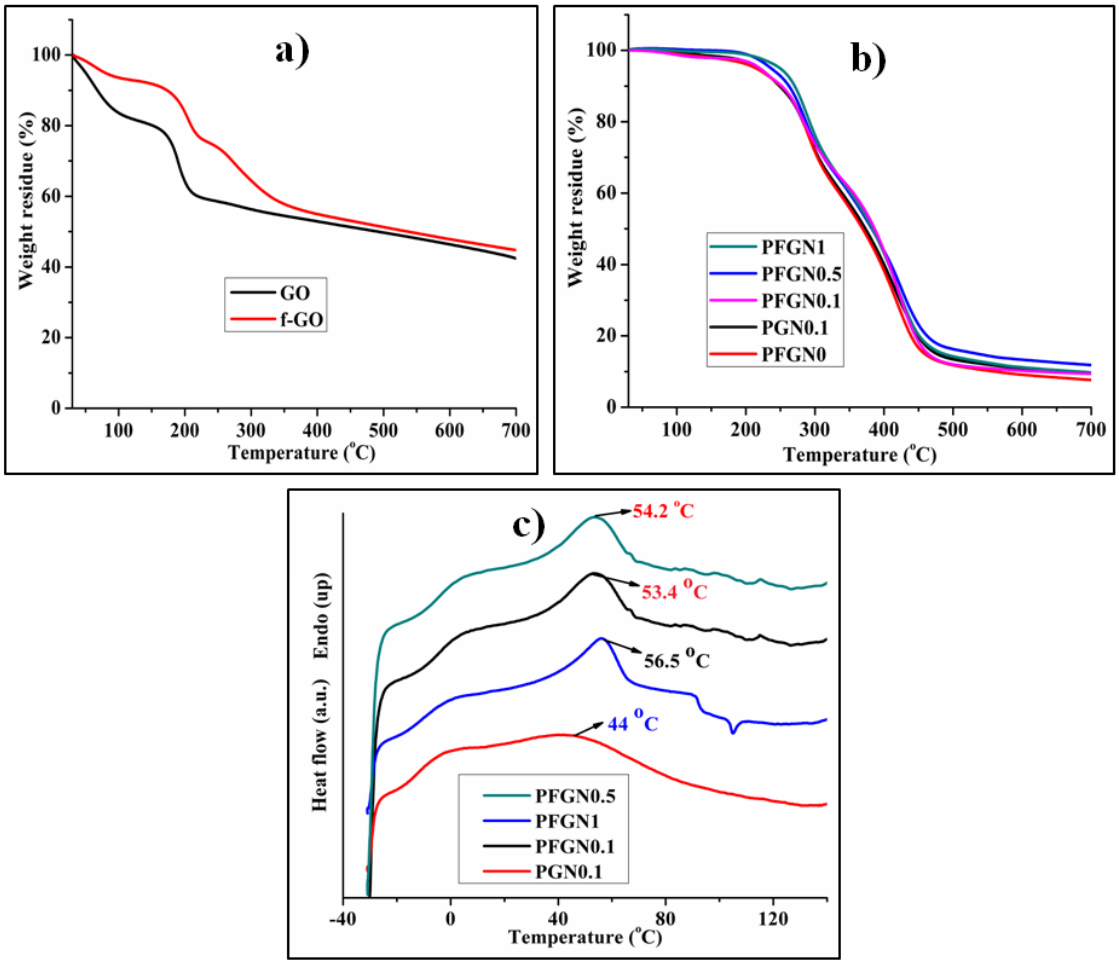

Figure 3.7: (a) TG thermograms of GO and f-GO, **(b)** TG thermograms and **(c)** DSC curves of the nanocomposites

T_g of the nanocomposite slightly increases after incorporation of f-GO and further increased with the loading of f-GO, indicating the mobility of polymer chains restriction. This restriction may be due to different physicochemical interactions of the polyester matrix with the nanomaterial and so hinder the movement of polymeric chains [27-29].

3.3.7. Biodegradation study

Most interestingly, apart from the enhancement in mechanical and thermal properties arising from incorporation of GO, the corresponding nanocomposite showed noticeable biodegradation behavior against *Pseudomonus aeruginosa* bacterial strain. The bacterial growth profiles for the nanocomposites obtained after 45 days are shown in **Figure 3.8**.

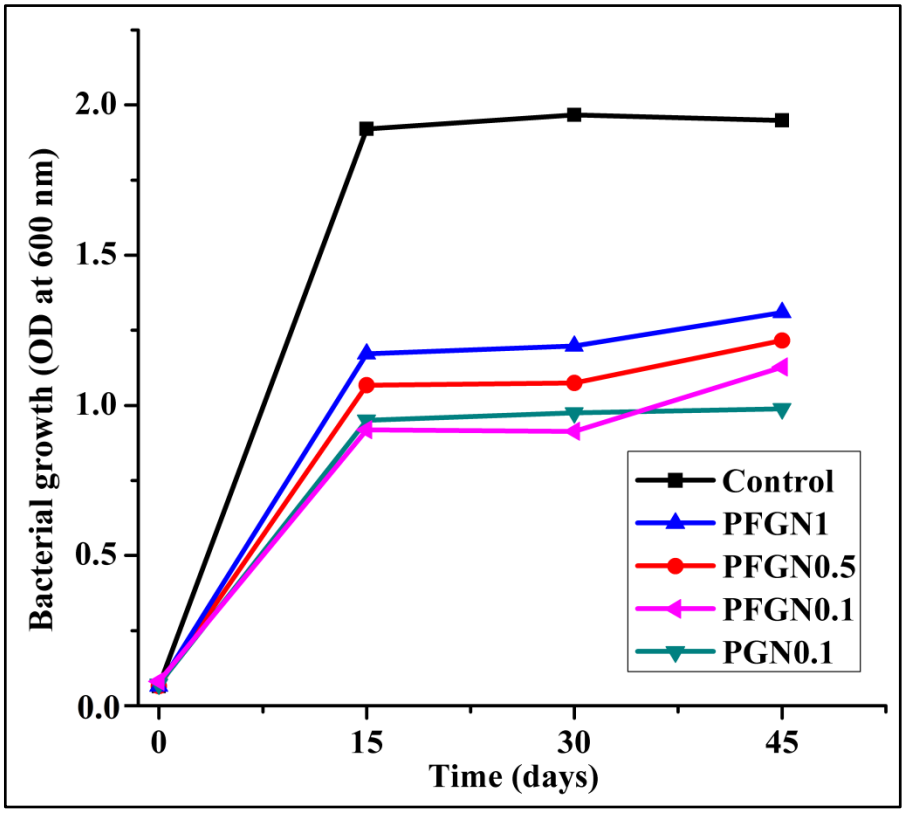

Figure 3.8: Bacterial growth curves for the nanocomposite against *Pseudomonas aeruginosa* bacterial strain

All the nanocomposites demonstrated significant bacterial growth against *Pseudomonas aeruginosa* on exposure of time. The factors like flexible moieties, amorphous nature of the polyester, polar linkages, and hydrophilic character are mainly responsible for such biodegradation [30, 31]. In case of polyester, the major mode of degradation is a hydrolytic random chain scission. The degradation involves various phenomena of

diffusion–reaction, including ester hydrolysis, solubilization of soluble species, water absorption and diffusion. Further, the ester cleavage is auto-catalyzed by end groups of carboxylic acid originally present in the polymer or nanomaterials or produced by hydrolytic degradation. The mechanism of biodegradation by the nanocomposite is schematically shown in **Scheme 3.6**. The representative SEM images (**Figure 3.9a-d**) of PFGN0.5 demonstrated the morphologies of the nanocomposite before and after biodegradation and established broad surface erosion after exposure.

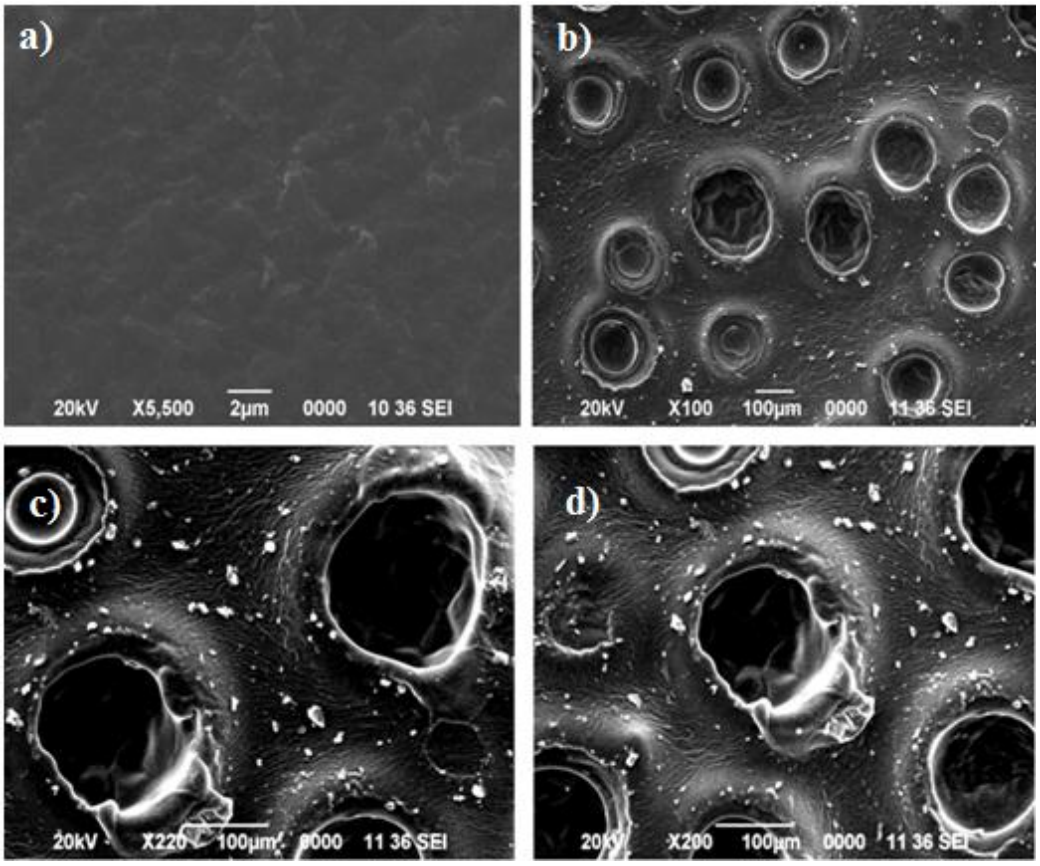

Figure 3.9: SEM micrographs of **(a)** control and **(b-d)** degraded thermosetting nanocomposite (PGGN0.5)

However, the degree of degradation of polyester in the vicinity of the graphene sheets is less compared to the bulk. GO itself is non-degradable, but its incorporation in polyester matrix has marginal effect on the overall biodegradability of the nanocomposite [20, 30]. This is due to increase of polar and flexible linkages including ester linkages which are prone to microbial attack. Further, the hydrophilic character and amorphous nature are the key factors responsible for this biodegradability [20]. Though GO reduces enzymatic hydrolysis rate in biodegradation [31], but in this case, the effect was not observed as no

enzyme was directly used during the biodegradation study. Further, due to functionalization of GO, this effect was not noticed though some enzymes may be released during the degradation process.

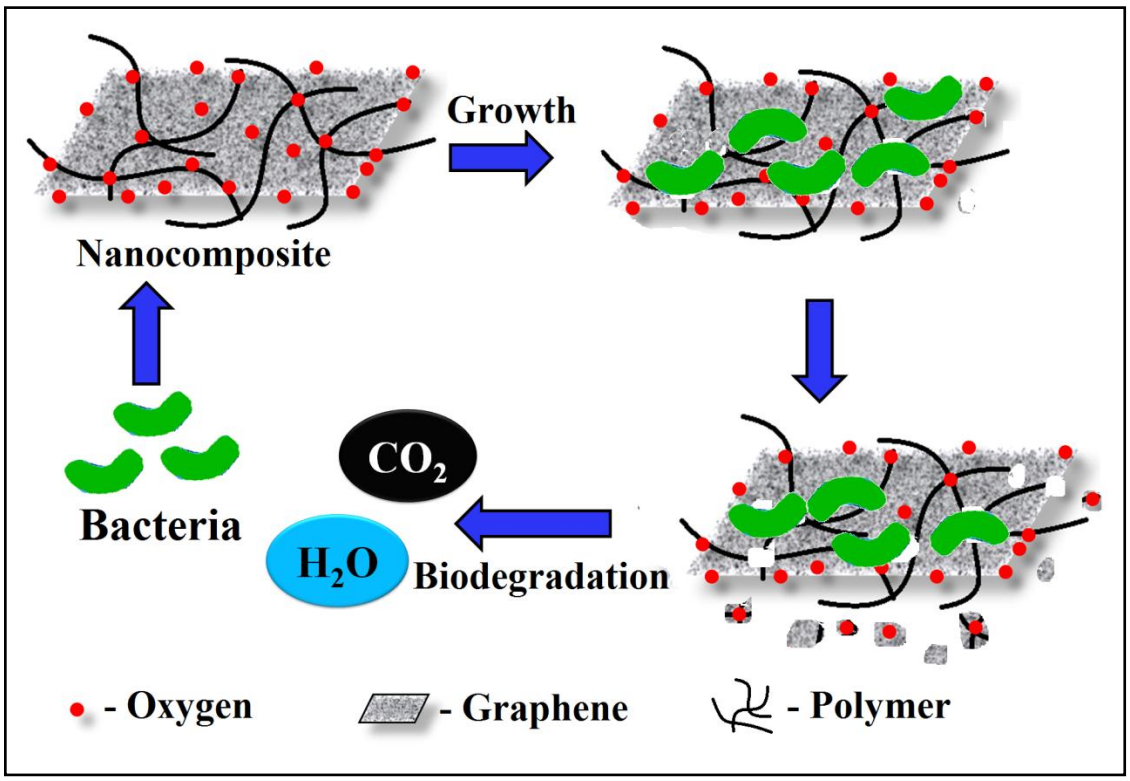

Scheme 3.6: Biodegradation of WHPE nanocomposite in presence of bacterial strain

3.3.8. Nanocomposite as a catalyst for Aza-Michael addition reaction

The nanocomposite was used as a catalyst for addition of an N-H bond across a multiple bond to give important nitrogen-containing compounds. The reaction between diethylamine and acrylonitrile was carried out using different catalyst systems (**Table 3.2**). The reaction was completed with the highest conversion (98%) within 3 min using PFGN1 as a catalyst. The yield was found to be higher than the reported GO based catalytic reaction [13]. The Aza-Michael addition reaction in the presence of GO is favorable because of the presence of oxygeneous functional groups on its surface which plays a role in the activation for this reaction. Thus, the observed higher yield of the reaction by the nanocomposite is due to the presence of huge number of functional groups than bare GO and f-GO. Further, the catalyst (PFGN1) concentration was optimized by varying its amount from 1.25×10^{-3} g to 0.05 g (**Table 3.3**, Entry 1-5). The enhancement in the yield of product was observed with the increase in the loading of the

catalyst amount. This is due to increase in GO concentration with increase in the loading of PFGN1 and hence increase in the number of oxygeneous functional groups showed the excellent result. Further, the reaction was studied using different amines with different α, β- unsaturated compounds under described conditions to obtain the desired products. The reactants were converted to the corresponding β-amino compounds without formation of any by-products with excellent yields within short reaction time. These results are given in **Table 3.4**. The obtained products were characterized by NMR spectroscopy and compared with the reported literature [32-34].

Table 3.2: Performance of different catalysts in Aza-Michael addition reaction

Entry	Catalyst	Yield (%)
1	[b]GO	97
3	[c]f-GO	98
4	[d]PFGN1	98.4
5	[e]WHPE	No reaction

[a] Reaction condition: Diethylamine (1 mmol, 73 mg) and acrylonitrile (1.2 mmol, 63 mg) were stirred at room temperature. [b]2.5×10^{-2} mg GO and [c]2.5×10^{-2} mg f-GO dispersion in 0.5 mL water, [d]2.5×10^{-3} g nanocomposite (PFGN1), [e]2.5×10^{-2} mg WHPE

Table 3.3: Effect of catalyst (PFGN1) loading for Aza-Michael addition reaction

Entry	*Catalyst loading (g)	Time (min)	Yield (%)
1	1.25×10^{-3}	3	97
2	2.5×10^{-3}	3	98.4
3	5×10^{-3}	3	99
4	1×10^{-2}	3	99.6
5	5×10^{-2}	3	100

Reaction condition: Diethylamine (1 mmol), acrylonitrile (1.2 mmol) and desired amount of catalyst were stirred at room temperature

1. 3-(diethylamino) propanenitrile, (Table 3.4, Entry 1)

^{1}H NMR (400 MHz, $CDCl_3$, δ): 2.67 (t), 2.40 (q), 2.30 (t) and 0.92 (t). The values are similar to the reported literature [32]. ^{13}C NMR (400 MHz, $CDCl_3$, δ): 119.6, 50, 47.2, 17.1 and 15.4 (**Figure 3.10**). These are supported by the Sci-finder results.

Table 3.4: Aza-Michael addition of different amines and α, β-unsaturated compounds in presence of PFGN1 as the catalyst

Entry	Amine	α, β-unsaturated compounds	Product	Reaction time (min)	Yield (%)
1	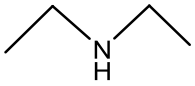	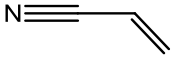	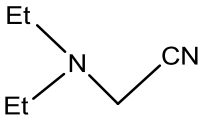	3	97
2	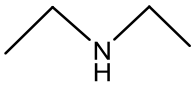	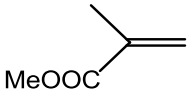	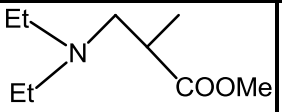	5	96
3	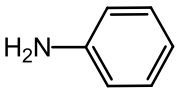	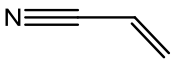	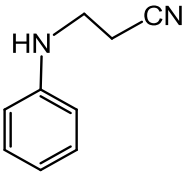	35	62

Reaction condition: Amine (1 mmol); α, β unsaturated compound (1.2 mmol)

2. 3-(diethyamino) 2-methyl methyl ester (Table 3.4, Entry 2)

^{1}H NMR (400 MHz, $CDCl_3$, δ): 1, 1.13, 2.42, 2.59, 2.84, 3.67. ^{13}C NMR (400 MHz, $CDCl_3$, δ): 175.8, 56, 51.2, 48, 38.5 15 and 13.4 (**Figure 3.11**). The values are supported by the Sci-finder results.

3. 3-(phenylamino)propanenitrile (Table 3.4, Entry 3)

^{1}H NMR (400 MHz, $CDCl_3$, δ): 2.58 (t), 3.47 (t) and 6.75-6.78 (m) and 7.2-7.25 (m). These are in accordance with the reported literature [32-34]. ^{13}C NMR (400 MHz, $CDCl_3$, δ): 147.7, 129.6, 117.7, 113.5, 40 and 19 (**Figure 3.12**). These values are supported by the Sci-finder results.

Further, recovery of the catalyst is key factor to determine whether it has potential for large scale application in industry or not. Thus, the recyclability of the catalyst was studied using the same Aza-Michael addition reaction of acrylonitrile and diethylamine as a model reaction and the results provided in the supporting information, **Table 3.5**. The catalyst was easily recovered by simple filtration after completion of the reaction. However, in the reported reaction by GO, the catalyst was recovered by extraction with dichloromethane from the reaction mixture [13]. Thus, the Aza-Michael addition reaction in the presence of

the nanocomposite has an added advantage than the reported GO nanoparticle [13].

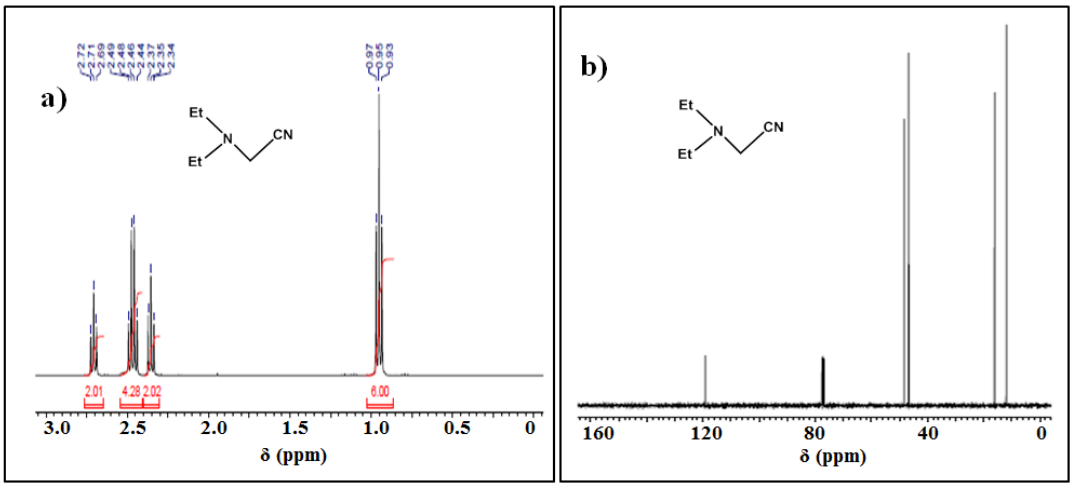

Figure 3.10: (a) ^{1}H and **(b)** ^{13}C NMR of 3-(diethylamino) propanenitrile

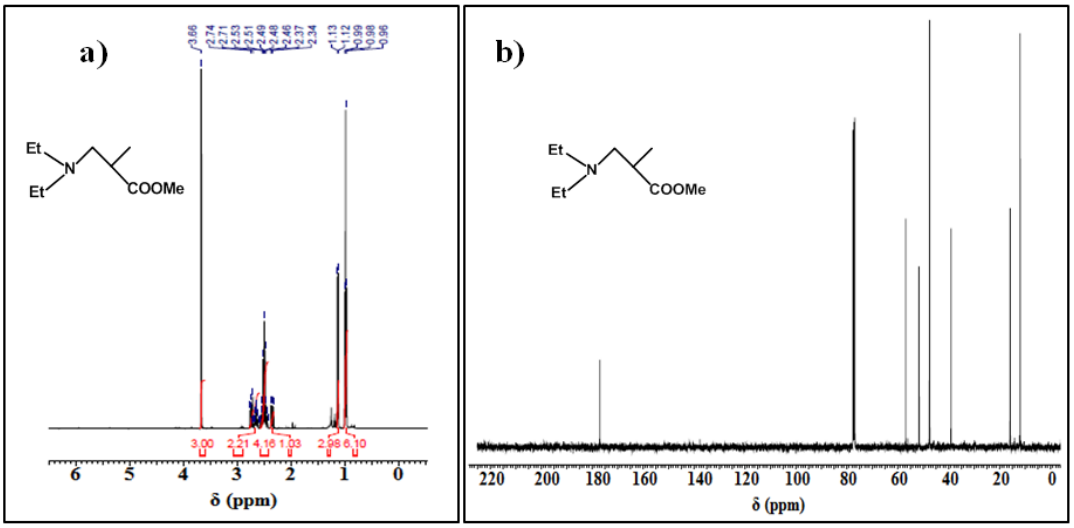

Figure 3.11: (a) ^{1}H and **(b)** ^{13}C NMR of 3-(diethyamino) 2-methyl methyl ester

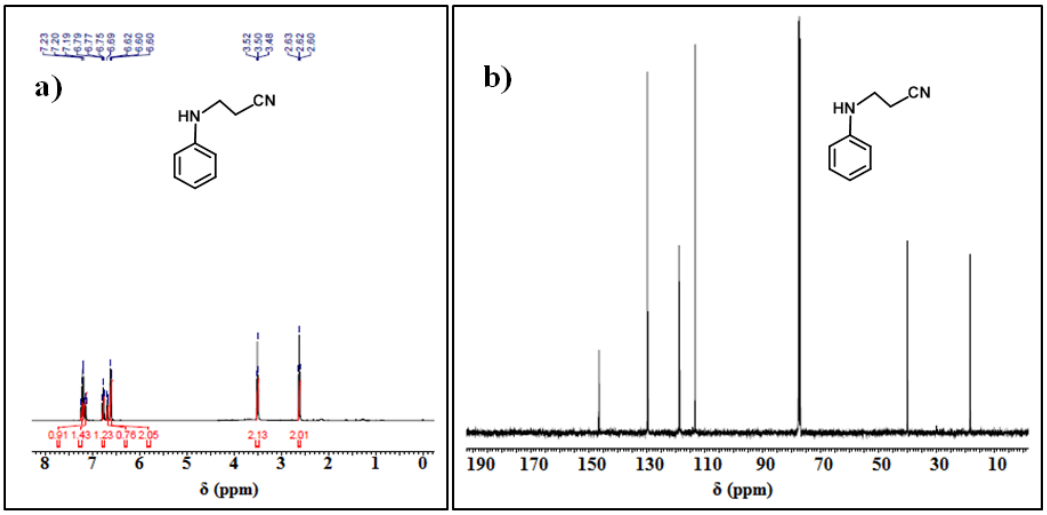

Figure 3.12: (a) ^{1}H and **(b)** ^{13}C NMR of 3-(phenylamino)propanenitrile

It is seen from **Table 3.5** that the yield of the product was found to be constant upto 4rd cycle during the recycling tests, establishing the efficient recyclability of the catalyst. Thus, the nanocomposite is an efficient heterogeneous catalyst for the synthesis of different amino-substituted compounds through Aza-Michael addition of α, β unsaturated compounds and amines. Further, it was also easily recoverable as well as recyclable with the constant catalytic activity.

Table 3.5: Results of the recycling experiment

Run	Time	Yield (%)
1	3	98.4
2	3	98.4
3	3	98.4
4	3	98.4
5	3	97.8

Reaction condition: Diethylamine (1mmol), acrylonitrile (1.2 mmol) and PFGN1 (2.5 × 10^{-3} g)

3.4. Conclusion

The present study established a facile, green and eco-friendly *in-situ* fabrication method to obtain a sustainable tough WHPE thermosetting nanocomposite with f-GO. More interestingly, this sustainable material was fabricated from bio-based raw materials and the process does not involve any additional catalyst and compatabilizing agent. Furthermore, such facile approach provides opportunity to produce high performing nanocomposite in a large-scale. The nanocomposite exhibited significant enhancement in mechanical and thermal properties at a low loading of nanomaterials. In addition, they showed biodegradation behavior towards *Pseudomonus aeruginosa* bacterial strain. They can be further utilized as an efficient heterogeneous catalyst for Aza-Michael addition reaction. Thus, the study stimulates new opportunities for fabrication of waterborne polymer/GO nanocomposite for a wide range of potential applications.

Reference

[1] Hamad, A. A., Hayyan, M., AlSaadi, M. A., and Hashim, M. A. Potential applications of deep eutectic solvents in nanotechnology. *Chemical Engineering Journal*, 273:551-567, 2015.

[2] Zhang, L., Zhang, H., and Guo, J. Synthesis and properties of UV-curable polyester-based waterborne polyurethane/functionalized silica composites and morphology of their nanostructured films. *Industrial & Engineering Chemistry Research*, 51(25):8434-8441, 2012.

[3] Kim, H. and Macosko, C. W. Morphology and properties of polyester/exfoliated graphite nanocomposites. *Macromolecules*, 41(9):3317-3327, 2008.

[4] Beg, M. D. H., Alam, A. K. M., Yunus, R. M., and Mina, M. F. Improvement of interaction between pre-dispersed multi-walled carbon nanotubes and unsaturated polyester resin. *Journal of Nanoparticle Research*, 17:53(1-13), 2015.

[5] Zhao, Y., Wang, F., Fu, Q., and Shi, W. Synthesis and characterization of ZnS/hyperbranched polyester nanocomposite and its optical properties. *Polymer*, 48(10):2853-2859, 2007.

[6] Thakur, S. and Karak, N. Ultratough, ductile, castor oil-based, hyperbranched, polyurethane nanocomposite using functionalized reduced graphene oxide. *ACS Sustainable Chemistry & Engineering*, 2(5):1195-1202, 2014.

[7] Potts, J. R., Dreyer, D. R., Bielawski, C. W., and Ruoff, R. S. Graphene-based polymer nanocomposites. *Polymer*, 52(1):5-25, 2011.

[8] Peng, S., Liu, C., and Fan, X. Surface modification of graphene oxide by carboxyl-group: Preparation, characterization, and application for proteins immobilization. *Integrated Ferroelectrics*, 163(1):42-53, 2015.

[9] McGrail, B. T., Mangadlao, J. D., Rodier, B. J., Swisher, J., Advinculab, R., and Pentzer, E. Selective mono-facial modification of graphene oxide nanosheets in suspension. *Chemical Communications*, 52(2):288-291, 2016.

[10] Bastiureaa, M., Rodeanua, M. S., Dimab, D., Murarescub, M., and Andreia, G. Thermal and mechanical properties of polyester composites with graphene oxide and graphite. *Digest Journal of Nanomaterial and Biostructure*, 10(2):521-533, 2015.

[11] Bora, C., Gogoi, P., Baglari, S., and Dolui, S. K. Preparation of polyester resin/graphene oxide nanocomposite with improved mechanical strength. *Journal of Applied Polymer Science*, 129(6):3432-3438, 2013.

[12] He, S., Petkovich, N. D., Liu, K., Qian, Y., Macosko, C. W., and Stein, A. Unsaturated polyester resin toughening with very low loadings of GO derivatives. *Polymer*, 110:149-157, 2016.

[13] Verma, S., Mungse, P. H., Kumar, N., Choudhary, S., Jain, S. L., Sain, B., and Khatri, P. Graphene oxide: An efficient and reusable carbocatalyst for aza-Michael addition of amines to activated alkenes. *Chemical Communications,* 47(47):12673-12675, 2011.

[14] Song, P., Cao, Z., Cai, Y., Zhao, L., Fang, Z., and Fu, S. Fabrication of exfoliated graphene-based polypropylene nanocomposites with enhanced mechanical and thermal properties. *Polymer*, 52(18):4001-4010, 2011.

[15] Zare, Y. Development of Halpin-Tsai model for polymer nanocomposites assuming interphase properties and nanofillers size. *Polymer Testing*, 51:69-73, 2016.

[16] Wang, X., Tan, D., Chu, Z., Chen, L., Chen, X., Zhao, J., and Chen, G. Mechanical properties of polymer composites reinforced by functionalized graphene prepared via direct exfoliation of graphite flakes in styrene. *RSC Advances,* 6(113):112486-112492, 2016.

[17] Thakur, S. and Karak, N. Green reduction of graphene oxide by aqueous phytoextracts. *Carbon*, 50(14):5331-5339, 2012.

[18] Brendan, T., McGrail, J. D., Mangadlao, B., Rodier, J., Swisher, J., Advinculab, R., and Pentzer, E. Selective mono-facial modification of graphene oxide nanosheets in suspension. *Chemical Communications,* 52(2):288-291, 2016.

[19] Song, S., Zhai, Y., and Yong, S. Bioinspired graphene oxide/polymer nanocomposite paper with high strength, toughness, and dielectric constant. *ACS Applied Materials & Interfaces,* 8(45):31264-31272, 2016.

[20] Baruah, P. and Karak, N. Bio-based tough hyperbranched epoxy/graphene oxide nanocomposite with enhanced biodegradability attribute. *Polymer Degradation and Stability*, 129:26-33, 2016.

[21] Hazarika, D. and Karak, N. Waterborne sustainable tough hyperbranched aliphatic polyester thermosets. *ACS Sustainable Chemistry & Engineering*, 3(10):2458-2468, 2014.

[22] Hu, L., Jiang, P., Zhang, P., Bian, G., Sheng, S., Huang, M., Bao, Y., and Xia, J. Amine-graphene oxide/waterborne polyurethane nanocomposites: Effects of different amine modifiers on physical properties. *Journal of Materials Science*, 51(18):8296-8309, 2016.

[23] Yadav, S. K. and Cho, J. W. Functionalized graphene nanoplatelets for enhanced mechanical and thermal properties of polyurethane nanocomposites. *Applied Surface Science*, 266:360-367, 2013.

[24] Abdullah, S. I. and Ansari, M. N. M. Mechanical properties of graphene oxide (GO)/epoxy composites. *HBRC Journal*, 11:151-156, 2015.

[25] Ouadila, B., Cherkaouib, O., Safia, M., and Zahouilya, M. Surface modification of knit polyester fabric for mechanical, electrical and UV protection properties by coating with graphene oxide, graphene and graphene/silver nanocomposites. *Applied Surface Science*, 414:292-302, 2017.

[26] Naebe, M., Wang, J., Amini, A., Khayyam, H., Hameed, N., Li, L. H., Chen, Y., and Fox, B. Mechanical property and structure of covalent functionalised graphene/epoxy nanocomposites. *Scientific Reports*, 4(1):4375, 2014.

[27] Chen, L., Zheng, K., Tian, X., Hu, K., Wang, R., Liu, C., Li, Y., and Cui, P. Double glass transitions and interfacial immobilized layer in in-situ synthesized poly (vinyl alcohol)/silica nanocomposites. *Macromolecules*, 43(2):1076-1082, 2010.

[28] Lu, H. and Nutt, S. Restricted relaxation in polymer nanocomposites near the glass transition. *Macromolecules*, 36(11):4010-4016, 2003.

[29] Li, X., Chen, L., Li, Q., Zhang, J., Su, Z., Zhang, X., Zheng K., and Tian, X. Double glass transitions in exfoliated poly (methyl methacrylate)/organically modified MgAl layered double hydroxide nanocomposites. *RSC Advances*, 6(104):101941-101947, 2016.

[30] Wang, X. W., Zhang, C. A., Wang, P. L., Zhao, J., Zhang, W., and Ji, J. H. Enhanced performance of biodegradable poly (butylene succinate)/graphene oxide nanocomposites via in situ polymerization. *Langmuir*, 28(18):7091-7095, 2012.

[31] Bikiaris, D. N., Nianias, N. P., Karagiannidou, E. G., and Docoslis, A. Effect of different nanoparticles on the properties and enzymatic hydrolysis mechanism of aliphatic polyesters. *Polymer Degradation and Stability*, 97(10):2077-2089, 2012.

[32] Borah, K. J., Phukan, M., and Borah, R. Aza-Michael addition of amines to α, β-unsaturated compounds using molecular iodine as catalyst. *Synthetic Communications*, 40(19):2830-2836, 2010.

[33] Ai, X., Wang, X., Liu, J., Ge, Z., Cheng, T., and Li, R. An effective Aza-Michael addition of aromatic amines to electron-deficient alkenes in alkaline Al_2O_3. *Tetrahedron*, 66(29):5373-5377, 2010.

[34] Bosica, G. and Abdilla, R. Aza-Michael mono-addition using acidic alumina under solvent less conditions. *Molecules*, 21(6):815(1-11), 2016.